33rd Annual International Conference of the IEEE EMBS
Boston, Massachusetts USA, August 30 - September 3, 2011

Parallel Independent Component Analysis using an Optimized Neurovascular Coupling for Concurrent EEG-fMRI Sources

Lei Wu, Tom Eichele, and Vince Calhoun

Abstract—**The complexity of the human brain and the limitation of any one imaging approach motivates the need for multimodal measurements to better understand cerebral processing. A very natural goal is to integrate electrophysiological and hemodynamic activity. Among them, concurrent EEG-fMRI studies have shown great promise for understanding intrinsic brain properties yet analyzing such data presents a significant methodological challenge. Here, we propose a multivariate parallel ICA decomposition incorporating dynamic neurovascular coupling for concurrent EEG-fMRI recordings. The goal of our algorithm is to fuse multimodal EEG-fMRI information and detect/interpret the relationship between electrophysiological and hemodynamic sources via a temporal neurovascular connection enhancement. We analyze the performance of the algorithm on a valid simulation based on real EEG and fMRI components (sources) from our previous works and a neurovascular coupling built from an extended 'balloon model'. The results from our simulations yield an accurate source tracking and linkage for concurrent EEG-fMRI, and provide a novel and efficient way to combine EEG and hemodynamic responses.**

I. Introduction

ONE of the essential problems in brain science is how electrical and hemodynamic signals that are acquired by e.g. electroencephalography (EEG) and functional magnetic resonance (fMRI) relate to each other during different states of cerebral activity. Scalp EEG samples the synchronous post-synaptic potentials in the cerebral cortex which lead to neuronal input processing, whereas blood-oxygenation-level dependent (BOLD) fMRI measures a delayed hemodynamic response to neuronal activity. Previous research has shown a linear relationship between local field potentials and multi-unit activity and the BOLD signal [1]. Methodologically, the motivation for combining electroencephalography (EEG) and functional magnetic resonance imaging (fMRI) is obvious. The advantage of EEG is millisecond temporal resolution and the ability to measure neuronal activity directly. In contrast, fMRI has excellent uniform spatial resolution but measures an indirect metabolic correlate of neuronal function - the BOLD signal, over a considerably longer time period of seconds. EEG and fMRI are complementary and thus an approach which combines fMRI and ERP can potentially draw on the strengths of each and provide additional information not afforded by either technique alone. The neurophysiologic and methodological motivations, along with the technical improvements that allow concurrent data acquisition, make combining EEG and fMRI a popular yet challenging ongoing effort that employs a variety of approaches.

Independent component analysis (ICA) is a widely used approach for blind source separation. In our previous work, we have applied ICA models to detect either single-modality sources of fMRI spatial maps (sICA), EEG time courses (tICA) and spectral information (spICA), or a 'post' coupling estimation (deconvolution) between the identified components [2-7]. In this paper, we propose a new multivariate approach to detect concurrent EEG-fMRI sources by fusing the neurovascular dynamics into a parallel ICA framework. Instead of tracking stationary projections independently from a single modality as in the aforementioned work, our algorithm here identifies the multivariate sources from EEG and fMRI data simultaneously based on a dynamic neurovascular coupling optimization.

The paper is organized as follows. Section II describes the mathematical model and the algorithm development. Then we evaluate the performance of our algorithm on a simulation based on a balloon model [8, 9] that generates realistic neurovascular couplings in section III. Experimental results are presented in section IV and section V concludes the paper.

II. Model and Algorithm

A. Infomax ICA

The basic idea underlying ICA is to assume that sources are independent and distributed sparsely. In this paper, we use an ICA approach based upon the infomax principle.

We start with the assumption of independence of the EEG rhythm and fMRI spatial sources approximately, respectively, using the following generative model for the data, which maps from sources to observed data feature (Equation (1)), where X is the observations of EEG or fMRI data; A is a linear mixing matrix, the loading parameters encoding the temporal pattern each source would cause over time; S contains the sources desired, i.e. EEG rhythms or fMRI spatial maps.

Manuscript received April 15, 2011. This work was supported in part by National Institutes of Health, under grants 1 R01 EB 006841, 1 R01 EB 005846 (VDC), and a grant from the L. Meltzer university fund 801616 (TE).

Lei Wu and Dr Vince Calhoun are with the Mind Research Network and Electrical and Computer Engineering Department, University of New Mexico, Albuquerque, NM 87106 USA (Contacts: lwu@mrn.org, vcalhoun@mrn.org; phone: 505-272-5165; fax: 505-272-8002).

Dr Tom Eichele is with the Department of Biological and Medical Psychology, University of Bergen, Bergen 5011, Norway (Contacts: tom.eichele@psybp.uib.no; phone: 47-555-86290).

$$X = AS \quad (1)$$

The goal of ICA is to find a linear mapping of W such that W approximates the inverse of A in order to determine the unmixed components U.

$$U = WX = WAS \quad (2)$$

The infomax algorithm employs a gradient ascent algorithm to maximize the entropy of the output of a single layer neural network. By infomax, we can estimate the unmixing matrix W in a maximum output entropy H(Y) sense encoded by the cumulative density function g, without knowing the sources. The resulting update equations for the algorithm to compute the W and the sources U are as follows [10, 11]:

$$\Delta W \propto \frac{\partial H(Y)}{\partial W} W^T W = \left[I + (1-2Y)U^T \right] W,\ Y = g(U) = \tanh(U) \quad (3)$$

where $W^T W$ is the natural gradient that rescales the gradient to simplify the learning rule and speed up the convergence. The transfer function g is chosen to be a logistic function to optimize the information flow.

B. Parallel ICA Framework for Concurrent EEG-fMRI

The aim is to construct EEG and fMRI ICA source localizations while using optimal neurovascular couplings as a constraint within the parallel EEG-fMRI ICA computation. Fig 1 shows our framework which includes three key parts.

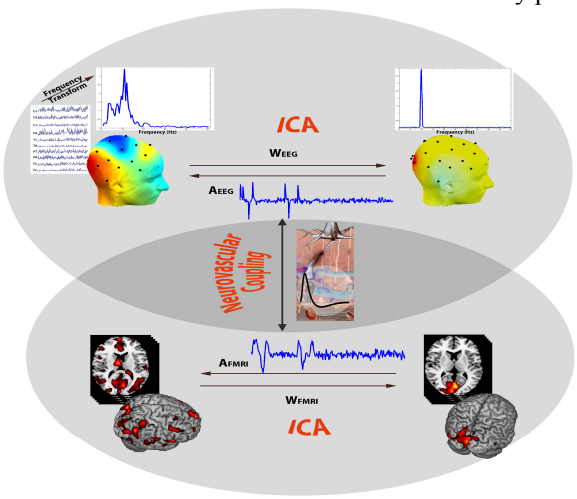

Fig. 1. Parallel EEG-fMRI ICA Model

1) ICA learning:

EEG: $W_E = \tilde{A}_E^{-1},\ U_E = W_E X_E;$

$$\Delta W_E \propto [I + (1 - 2Y_E) U_E^T] W_E,\ \tilde{W}_E = W_E + \Delta W_E \quad (4)$$

FMRI: $W_F = \tilde{A}_F^{-1},\ U_F = W_F X_F;$

$$\Delta W_F \propto [I + (1 - 2Y_F) U_F^T] W_F,\ \tilde{W}_F = W_F + \Delta W_F \quad (5)$$

$\tilde{A}_E$ and $\tilde{A}_F$ are the EEG and fMRI time-course 'features' and U is the estimation of the sources.

2) Neurovascular optimization:

$$A_E = \tilde{W}_E^{-1},\ A_F = \tilde{W}_F^{-1},\ \left\{ \tilde{A}_E, \tilde{A}_F \right\} = \max \left\{ NCF\left(A_E, A_F \right) \right\} \quad (6)$$

$\tilde{W}_E$ and $\tilde{W}_F$ are the EEG and fMRI demixing factors obtained from the ICA learning. NCF represents a neurovascular coupling function between EEG and fMRI, which will be discussed next.

3) Balance verification:

This part is semi-hidden. Our model simultaneously optimizes both the maximum independence of EEG and fMRI sources in addition to the maximum neurovascular coupling by tuning the learning rates for the correlation and crosschecking the impacts on the entropy maximization. Additionally we include bias correction, annealing to avoid overfitting and stability control, *et al.*, to prevent one of the criteria from dominating.

C. Neurovascular Optimization

For concurrent EEG-fMRI data, an intuitive linkage between the estimated parallel ICA sources is a neurovascular coupling model.

A dynamic EEG-fMRI neurovascular optimization algorithm is developed here to integrate two different modalities as well as to connect the two ICA models. Realistic neurovascular modeling involves many nonlinear/linear factors [9], which will be discussed in the following simulation. In fMRI, a linear convolution approach to determine a hemodynamic response function (HRF) is commonly used [12-14]. However, the HRF as a linear representation of neurovascular coupling between EEG and fMRI can vary between brain regions, brain rhythms and subjects [15-17]. Previous concurrent EEG-fMRI works indicate the hemodynamic temporal delay is a main ingredient of neurovascular correlates [18]. Here we use a cross-correlation term with time lags to detect the hemodynamic delay and determine the HRF using the following canonical form.

$$\left\{ \tau^* \mid \tau = k \right\} = \arg\max_{\tau} \left\{ XCorr_{A_e, A_f}(\tau), \mid \tau \mid < D_{MAXLAG} \right\}$$

$$XCorr_{A_e, A_f}(\tau) = \frac{K_{A_e, A_f}(\tau)}{\sigma_{A_e} \sigma_{A_f}} = \frac{E[(\hat{A}_{e,\tau} \cdot \hat{A}_f]}{\sigma_{A_e} \sigma_{A_f}},\ \hat{A} = A - \mu_A \quad (7)$$

$$HRF_\tau = \Gamma\left(u_{peak}, h_{peak}(\tau), l_{peak} \right) - \Gamma_{undershoot}$$

where A_e and A_f are the column vectors of the mixing matrices A_E and A_F (time-course features) from EEG and fMRI separately. $K(\tau)$ is the covariance on lag τ. E is the expectation. $A_{e,\tau}$ is A_e lagged τ, where the $\wedge$ denotes removing the mean μ_A, σ is the standard deviation. The HRF is computed by two gamma density functions, where the delay τ controls the HRF peak timing. The rest parameters are set as default in the canonical form.

Then we apply a correlation between 'HRF-convolved' EEG and fMRI time courses as our NCF. To reach the maximum of the NCF, i.e. maximizing the correlation, a gradient ascent is again performed.

$$NCF(A_E, A_F) = Corr\left(A_e^*, A_f \right),\ A_e^* = A_e * HRF_{\tau^*} \quad (8)$$

To determine the $\max \{ Corr(A_e^*, A_f) \}$ we use:

$$\Delta A_e \propto \frac{\partial Corr\left(A_e^*, A_f \right)}{\partial A_e}$$

$$
\begin{aligned}
&= \frac{1}{\sigma_{A_e^*}\sigma_{A_f}} \cdot \frac{\partial K_{A_e^*,A_f}}{\partial A_e} + \frac{K_{A_e^*,A_f}}{\sigma_{A_f}} \cdot \frac{\partial \sigma^{-1}_{A_e^*}}{\partial A_e} \\
&= \left(\frac{A_f - \mu_{A_f}}{\sigma_{A_f}} - \frac{A_e^* - \mu_{A_e^*}}{\sigma_{A_e^*}} Corr\left(A_e^*, A_f\right) \right) \bullet \frac{HRF_{\tau^*}(0)}{(N-1)\cdot\sigma_{A_e^*}} \\
&\propto \overline{A_f} - \overline{A_e^*} Corr\left(A_e^*, A_f\right) \\
\tilde{A}_e &= A_e + sign(Corr\left(A_e^*, A_f\right))\Delta A_e
\end{aligned}
\tag{9}
$$

Similarly,

$$
\begin{aligned}
\Delta A_f &\propto \overline{A_e} - \overline{A_f^*} Corr\left(A_e^*, A_f\right) \\
\tilde{A}_f &= A_f + sign(Corr\left(A_e^*, A_f\right))\Delta A_f
\end{aligned}
\tag{10}
$$

$\overline{A_e^*}$ and $\overline{A_f}$ are normalized A_e^*, A_f. By adjusting the $\frac{HRF_{\tau^*}(0)}{(N-1)\cdot\sigma_{A_e^*}}$ into the learning rate, the NCF learning rules are simplified as Equations (9) and (10). It also very easy to understand, as the direction of A_e is controlled by A_f and their correlation; vice versa. The sign(.) is to make sure it reaches the absolute maximum of either the positive or negative correlation.

III. SIMULATION DESIGN

To test the performance of our algorithm, we devise a realistic simulation for the concurrent EEG-fMRI process (Fig. 2).

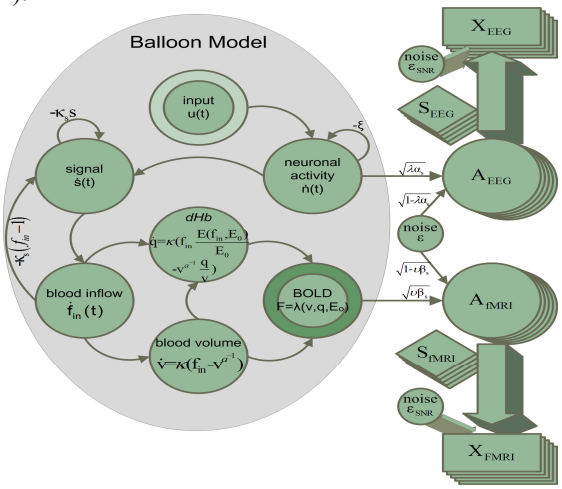

Fig. 2. Simulation Model Flowchart

Recent studies have provided an exceptional modeling approach for forward models of neurovascular coupling that are neurophysiologically grounded [19-22]. Among them, the "balloon model" is quite promising and well developed [8]. Here in Fig. 2 we simulate the neuroelectrical signals and their hemodynamic responses based on an extended balloon model [9]. The balloon model deals with the mesoscopic link between blood flow and BOLD signal. The extended model covers the dynamic coupling of synaptic activity and flow a complete model, relating induced changes in neuronal activity to BOLD signal. To simulate the concurrently measured whole brain EEG-fMRI signal, we further extend it by linearly mixing with EEG rhythm patterns S_{EEG} and fMRI spatial patterns S_{FMRI} with susceptibility and signal-to-noise controls (Equation (11)), with the parameters of α_s, β_s, α_x β_x and λ, ν, δ η respectively. The behavior of this entire model provides us a realistic brain signal simulation in terms of the concurrent EEG-fMRI.

$$
\begin{aligned}
A_{EEG}(s,t) &= \sqrt{\lambda\alpha_s}\cdot n_s(t) + \sqrt{1-\lambda\alpha_s}\cdot\varepsilon_s(t) \\
A_{FMRI}(s,t) &= \sqrt{\upsilon\beta_s}\cdot F_s(t) + \sqrt{1-\upsilon\beta_s}\cdot\varepsilon_s(t) \\
X_{EEG}(t) &= \sqrt{\delta\alpha_x}\sum_s A_{EEG}(s,t) S_{EEG}(s,P_{EEG}) + \sqrt{1-\delta\alpha_x}\cdot\varepsilon_x(t) \\
X_{FMRI}(t) &= \sqrt{\eta\beta_x}\sum_s A_{FMRI}(s,t) S_{FMRI}(s,P_{FMRI}) + \sqrt{1-\eta\beta_x}\cdot\varepsilon_x(t)
\end{aligned}
\tag{11}
$$

IV. EXPERIMENTS AND RESULTS

We generate simultaneous EEG and fMRI datasets by the model in part III. Source patterns for EEG and fMRI are selected as five EEG rhythms (delta, theta, alpha, beta, gamma) and five major neuronal regions (PCC, Occipital, frontal, DMN and temporal lobe) respectively, based on our previous work [17]. After generating the time series that are generated by the balloon model, random Gaussian noise (SNR=5) is added.

The parallel ICA results are indicated in Fig 3. We simulate 5 ICs which are used as the ground truth. Each IC contains EEG rhythm pattern recovery (1st column; thick blue line; black dot line as the original mean); fMRI spatial pattern recovery (2nd column top; bottom as the original); EEG and fMRI time course recovery (3rd and 4th columns; blue as the original balloon model outputs; red as simulated EEG and fMRI time series; black as recovery). Overall, the parallel ICA successfully matches the source pattern linkages and neurovascular couplings, with a high accuracy of correlation between 0.771~0.982.

V. CONCLUSION

In this paper a new parallel ICA algorithm for simultaneous EEG-fMRI recording was introduced and tested in a neurovascular simulation. The results support that our method can detect coherent linked hidden sources among concurrent EEG-fMRI measurements. The algorithm contains a dynamic neurovascular coupling detection and optimization; and appears to be robust to noise, a limitation of other existing methods such as inverse calculation or deconvolution. Future directions include further improving the NCF estimation, e.g. using partial least square instead of correlation; using more information to improve the estimate of HRFs, e.g. one for peak delay and one for undershoot; estimating the nonlinear cascade between EEG and fMRI coupling. Our results demonstrate that data-driven methods can be successfully combined with model-driven methods. We believe that these two major approaches for EEG-fMRI research are complementary and should be used together. For instance, applying neurophysiologic models, such as the balloon model, into the coupling optimization in our parallel ICA model may allow us track the nonlinear neurovascular relationship that is known to exist.

REFERENCES

[1] N. K. Logothetis, J. Pauls, M. Augath, T. Trinath, and A. Oeltermann, "Neurophysiological investigation of the basis of the fMRI signal," Nature, vol. 412, pp. 150-157, 2001.

[2] V. D. Calhoun, T. Adali, G. D. Pearlson, and J. J. Pekar, "A Method for Making Group Inferences from Functional MRI Data Using Independent Component Analysis," Human Brain Mapping, vol. 14, pp. 140-151, 2001.

[3] T. Eichele, V. D. Calhoun, and S. Debener, "Mining EEG-fMRI using independent component analysis," Int J Psychophysiol, vol. 73, pp. 53-61, 2009.

[4] L. Wu, T. Eichele, and V. Calhoun, "Reactivity of hemodynamic responses and functional connectivity to different states of alpha synchrony: a concurrent EEG-fMRI study," Neuroimage, vol. 52, pp. 1252-1260, 2010.

[5] L. Wu, T. Eichele, and V. Calhoun, "A Multi-subject Parallel ICA Method for Simultaneous EEG-fMRI Resting Data Analysis," in HBM 17th Annual Meeting, , Quebec, Canada: HBM, 2011.

[6] L. Wu, V. Calhoun, and T. Eichele, "Intrinsic connectivity networks in Eyes Open vs. Eyes Closed EEG-fMRI," in HBM 17th Annual Meeting Quebec, Canada: HBM, 2011.

[7] V. D. Calhoun, L. Wu, K. A. Kiehl, T. Eichele, and G. Pearlson, "Aberrant Processing of Deviant Stimuli in Schizophrenia Revealed by Fusion of FMRI and EEG Data," Acta Neuropsychiatrica, vol. 22, pp. 127-138, 2010.

[8] R. B. Buxton, E. C. Wong, and L. R. Frank, "Dynamics of blood flow and oxygenation changes during brain activation: the balloon model." vol. 39: New York: Academic Press, 1998, pp. 855-864.

[9] K. J. Friston, A. Mechelli, R. Turner, and C. J. Price, "Nonlinear responses in fMRI: the Balloon model, Volterra kernels, and other hemodynamics," Neuroimage, vol. 12, pp. 466-477, 2000.

[10] A. J. Bell and T. J. Sejnowski, "An information-maximization approach to blind separation and blind deconvolution," Neural Comput, vol. 7, pp. 1129-59, 1995.

[11] S. Amari, "Natural gradient learning for over- and under-complete bases In ICA," Neural Comput, vol. 11, pp. 1875-1883, 1999.

[12] R. I. Goldman, J. M. Stern, J. Engel Jr, and M. S. Cohen, "Simultaneous EEG and fMRI of the alpha rhythm," Neuroreport, vol. 13, pp. 2487-2492, 2002.

[13] M. Moosmann, T. Eichele, H. Nordby, K. Hugdahl, and V. D. Calhoun, "Joint independent component analysis for simultaneous EEG-fMRI: principle and simulation," Int J Psychophysiol, vol. 67, pp. 212-221, 2008.

[14] H. Laufs, A. Kleinschmidt, A. Beyerle, E. Eger, A. Salek-Haddadi, C. Preibisch, and K. Krakow, "EEG-correlated fMRI of human alpha activity," Neuroimage, vol. 19, pp. 1463-1476, 2003.

[15] J. C. de Munck, S. I. Gonçalves, L. Huijboom, J. P. A. Kuijer, P. J. W. Pouwels, R. M. Heethaar, and F. H. Lopes da Silva, "The hemodynamic response of the alpha rhythm: An EEG/fMRI study," NeuroImage, vol. 35, pp. 1142-1151, 2007.

[16] J. C. de Munck, S. I. Goncalves, R. Mammoliti, R. M. Heethaar, and F. H. Lopes da Silva, "Interactions between different EEG frequency bands and their effect on alpha-fMRI correlations," Neuroimage, vol. 47, pp. 69-76, 2009.

[17] L. Wu, T. Eichele, and V. Calhoun, "Alpha Hemodynamic Responses in Eyes Open vs. Eyes Closed Resting State EEG-fMRI," in HBM 16th Annual Meeting Barcelona, Spain: HBM, 2010.

[18] F. Bießmann, F. Meinecke, A. Gretton, A. Rauch, G. Rainer, N. K. Logothetis, and K.-R. Müller, "Temporal kernel CCA and its application in multimodal neuronal data analysis," Machine Learning, vol. 79, pp. 5-27, 2009.

[19] R. G. Shulman, F. Hyder, and D. L. Rothman, "Cerebral energetics and the glycogen shunt: neurochemical basis of functional imaging," Proc Natl Acad Sci U S A, vol. 98, pp. 6417-6422, 2001.

[20] J. J. Riera, X. Wan, J. C. Jimenez, and R. Kawashima, "Nonlinear local electrovascular coupling. I: A theoretical model," Human Brain Mapping, vol. 27, pp. 896-914, 2006.

[21] J. J. Riera, J. C. Jimenez, X. Wan, R. Kawashima, and T. Ozaki, "Nonlinear local electrovascular coupling. II: From data to neuronal masses," Human Brain Mapping, vol. 28, pp. 335-354, 2007.

[22] R. C. Sotero and N. J. Trujillo-Barreto, "Biophysical model for integrating neuronal activity, EEG, fMRI and metabolism," Neuroimage, vol. 39, pp. 290-309, 2008.

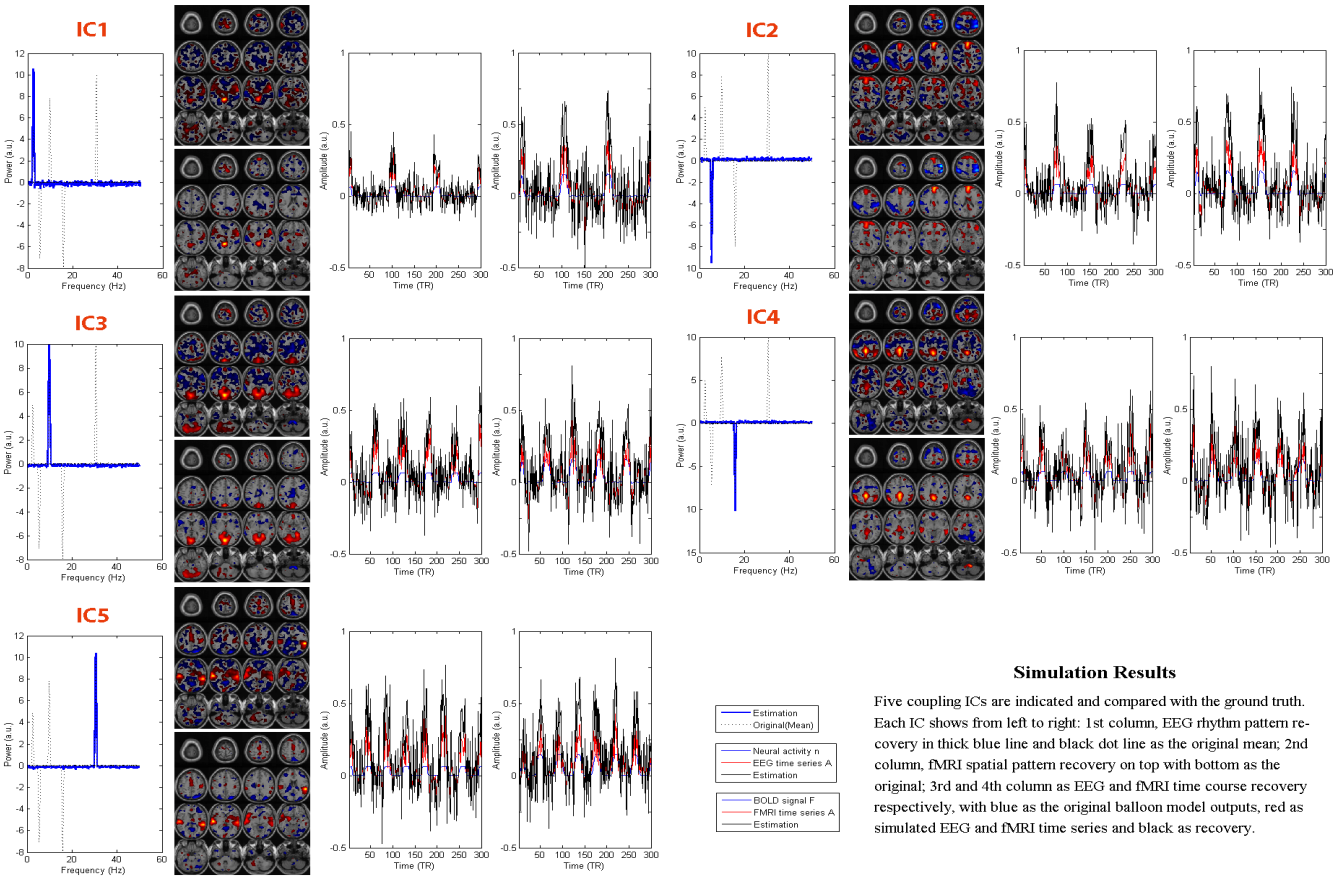

Fig. 3 Simulation Results